Supplementary Information for

The lupus autoantigen La is an Xist-binding RNA chaperone involved in Xist folding and cloud formation

Norbert Ha[2,3], Nan Ding[1,3], Ru Hong[2], Rubing Liu[2], Xavier Roca[2], Yingyuan Luo[1], Xiaowei Duan[1], Xiao Wang[1], Li-Feng Zhang[2,4,*] & Lingyi Chen[1,*]

Lingyi Chen, Li-Feng Zhang
Email: lingyichen@nankai.edu.cn, ZLF02472@gmail.com

This PDF file includes:

Other supplementary materials for this manuscript include the following:

Supplementary Information text

Comparison of the candidate proteins of this study with previous studies:

All 81 proteins identified by Chu et al(1) (annotated as C in Table S2) and all 10 proteins identified by McHugh et al(2) (annotated as N in Table S2) were compared with the candidate proteins identified in this study. The study of Minajigi et al(3) (annotated as S in Table S2) identified more than 700 proteins. The top 93 proteins ranked by "log2_avgFX/avgMX" were selected and compared with the candidate proteins identified in this study.

Definition of functional groups:

The candidate proteins are classified into each functional group based on the protein's function description in Uniport and NCBI gene.

Nuclear actin and related proteins:

1) The protein is myosin, unconventional myosin or myosin-binding.
2) The protein is actin-like, actin-related, actin-binding, actin filament binding, actin-crosslinking or regulates actin dynamics and organization.

Chromatin and related proteins:

1) The protein is involved in regulating chromatin structure, recruiting chromatin-remodeling enzymes, mediating nuclear import of histones and nucleosome assembly.
2) The protein possesses, recruits or regulates histone modification enzyme activities.
3) The protein binds to histones or modified histones.
4) The protein is a histone or histone variant.

DNA and RNA binding:

1) The protein is RNA-binding or DNA-binding.

Nuclear RNPs, ribosomal and nucleolar proteins:

1) The protein is a nuclear RNP.
2) The protein is a ribosomal protein.
3) The protein is a nucleolar protein.
4) The protein is involved in processing rRNA.

Membrane Proteins:

1) The protein is associated with plasma membrane, mitochondria membrane, trans-Golgi network and vesicle trafficking

Supplementary Materials and Methods

FLAG-out

Three 15 cm dishes of ES cells were cultured in differentiation medium supplemented with doxycycline for 48 hours. Cells were washed with ice cold PBS once and crosslinked with 0.4 J/cm^2 of $UV_{254\ nm}$. Cells were then harvested by trypsin treatment and lysed in 3 ml of lysis buffer (50 mM Tris HCl, pH 7.4; 150 mM NaCl; 1% TRITON X-100; 5% glycerol; supplemented with protease inhibitors and RNase Inhibitor). Cell lysates were first digested with TURBO DNase (Ambion). After centrifugation, supernatants were collected for co-IP experiment using anti-Flag M2 beads (Sigma). Elution of IPed proteins from anti-Flag M2 beads was achieved by 5 rounds of RNA/DNA digestion using 250 U of Benzonase (Millipore, #71206-3) for 2 h at 37°C. The eluted proteins were concentrated in a speed-vacuum to a final volume about 60 μl. One third of the elusions were separated on a 10% SDS-PAGE gel and stained by colloidal blue. The rest of the elusions were run on another 10% SDS-PAGE gel shortly, and the unresolved gel slices were subjected to mass spectrometry analysis.

Cell Survival Assay

Doxycycline treatment of 1 μg/ml was used throughout the study. G418 (ThermoFisher) treatment was carried out at 250 μg/ml. If ES cells were cultured as undifferentiated ES cells, Alkaline phosphatase (AP) staining (Vector Laboratories) was used at the end of the assay for counting the cells. ImageJ (4) was used to analyze AP staining data.

shRNA knockdown

An shRNA system (OligoEngine, pSUPER RNAi System) was used. The following shRNA sequences were designed against *Mybbp1a* (5'-CCGGAGTGTATTTGGTCATAT-3'), *Tardbp* (5'-GAATATGAAACCCAAGTGAAA-3'), *Ssb*-1(5'-GAGAAGATTTACACTTCCTTT-3'), and *Ssb*-2 (5'-GAACAGATCAAATTGGATGAA-3'). 300 μg/ml Hygromycin B (ThermoFisher; 10687010) was used to select stably transfected cell lines. Single surviving ES cell colonies were picked and the knockdown efficiency was validated using RT-qPCR.

Quantitative RT-PCR

Total RNA was isolated by TRIzol (Life technologies). cDNA was synthesized using iScript reverse transcription kit (170-8840, Bio-Rad). The real-time PCR was carried out on the CFX Connect real-time PCR system (Bio-Rad) using the SsoAdvanced Universal SYBR Green Supermix (Bio-Rad). The following PCR primers were used: Actb (F: 5'- ACTGCCGCATCCTCTTCCTC-3', R: 5'-CCGCTCGTTGCCAATAGTGA-3'); Gapdh (F: 5'-CCAATGTGTCCGTCGTGGAT-3', R: 5'-TGCCTGCTTCACCACCTTCT-3'); Mybbp1a (F: 5'-GCCGCGAGTTCTTGGACTT-3', R: 5'-ATCTCCGAATCATTGGGCCTT-3'); Tardbp (F: 5'- AATCAGGGTGGGTTTGGTAACA-3', R: 5'-GCTGGGTTAATGCTAAAAGCAC-3'); Ssb (F: 5'-ACCAAGCAGACCACTCCCTG-3', R: 5'-GGTGGCGTCAGTTGGGAAAC-3'); Cybb (F: 5'-TGTGGTTGGGGCTGAATGTC-3', R: 5'-CTGAGAAAGGAGAGCAGATTTCG-3'); Xiap (F: 5'-CGAGCTGGGTTTCTTTATACCG-3', R: 5'-GCAATTTGGGGATATTCTCCTGT-3'); Il2rg (F: 5'-CTCAGGCAACCAACCTCAC-3', R: 5'-GCTGGACAACAAATGTCTGGTAG-3'); Mecp2 (F: 5'-CAGGGAGGAAAAGTCAGAAGACC-3', R: 5'-AATGGTGGGCTGAAGGTTGTA-3'); Hprt (F: 5'-GATTAGCGATGATGAACCAGGTT-3', R: 5'-CCTCCCATCTCCTTCATGACA-3'); Gpc4 (F: 5'-GGCAGCTGGCACTAGTTTG-3', R: 5'-AACGGTGCTTGGGAGAGAG-3'); Neomycin (F: 5'-GGCTATTCGGCTATGACTGGGC-3', R: 5'-GCAGTTCATTCAGGGCACCG-3'); tdTomato (F: 5'-CCGACATCCCCGATTACAAGAAGC-3', R: 5'-TTGTAGATCAGCGTGCCGTC-3').

Padlock probe SNP capture

The padlock probe library design and padlock SNP capture procedure were performed as previously described (5). Briefly, each reaction was carried out in 20 μl volume containing 1 unit Ampligase (A3210K, Epicenter), 1 unit Phusion High-Fidelity DNA Polymerase (M0530, New England BioLabs), 1 × Phusion High-Fidelity DNA Polymerase buffer, 10 nM dNTP. cDNA was generated using SuperScript III first-strand synthesis system (18080-051, Life Technologies). Two hundred nanograms of single-stranded cDNA and 2 pmol padlock probe were used in each reaction. Nicotinamide adenine dinucleotide (Sigma; N0632) was provided in each reaction at a final concentration of 0.5 mM.
The multiplexed sequencing libraries were PCR amplified in a real-time PCR system (CFX Connect, Bio-Rad) using the following primers: CA-2-RA.Miseq (5′-AATGATACGGCGACCACCGAGATCTATCGGCTACACGCCTATCGGGAAGCTGAAG-3′); CA-2-

FA.Indx7Sol (5′-
CAAGCAGAAGACGGCATACGAGATGATCTGCGGTCTGCCATCCGACGGTAGTGT-3′); CA-2-
FA.Indx45Sol (5′-
CAAGCAGAAGACGGCATACGAGATCGTAGTCGGTCTGCCATCCGACGGTAGTGT-3′); CA-2-
FA.Indx76Sol (5′-
CAAGCAGAAGACGGCATACGAGATAATAGGCGGTCTGCCATCCGACGGTAGTGT-3′); CA-2-
FA.Indx91Sol (5′-
CAAGCAGAAGACGGCATACGAGATACATCGCGGTCTGCCATCCGACGGTAGTGT-3′); CA-2-
FA.Indx92Sol (5′-
CAAGCAGAAGACGGCATACGAGATTCAAGTCGGTCTGCCATCCGACGGTAGTGT-3′); CA-2-
FA.Indx93Sol (5′-
CAAGCAGAAGACGGCATACGAGATATTGGCCGGTCTGCCATCCGACGGTAGTGT-3′). The following sequencing primers were used: Read1.Miseq (5′-
ATCGGCTACACGCCTATCGGGAAGCTGAAG-3′); IndexRead (5′-
ACACTACCGTCGGATGGCAGACCG-3′). Sequencing was carried out on an Illumina NextSeq system.

ATAC-seq

Trypsinized cells were pelleted and washed with PBS. A total of 55,000 cells were lysed using cold lysis buffer (10 mM Tris-Cl, pH 7.4, 10 mM NaCl, 3 mM $MgCl_2$, 0.1% (v/v) Igepal CA-630) for 3 mins and centrifuged at 500 ×*g* at 4 °C for 10 mins. Pellets were resuspended with transposition reaction mix (2.5 µL TD, 2.5 µL TDE1, 22.5 µL nuclease-free water) (Nextera DNA library preparation kit, Cat No. FC-121-1030) and incubated in Thermomixer at 37° for 30 min with 1000 rpm. Transposed DNA samples were purified with Qiagen MinElute PCR purification kit (Cat No.: 28006) and eluted with 20 µL elution buffer from Qiagen MinElute PCR purification kit. The purified transposed DNA fragments were amplified by PCR. Each reaction was carried out in 50 µL volume containing 20 µL of transposed DNA, 2.5 µL of 25 µM Ad1_noMX primer (6), 2.5 µL of 25 µM Ad2.* indexing primer (6), 25 µL of NEBNext High-Fidelity 2× PCR Master Mix (Cat. No. M0541) with the following cycles: 1 cycle: 5 min at 72 °C, 30 s at 98 °C and 5 cycles: 10 s at 98 °C, 30 s at 63 °C, 1 min at 72 °C. Quantitative PCR was carried out on the PCR products to calculate the additional PCR cycles required before reaching saturation. Each qPCR reaction was carried out in 15 µL volume containing 5 µL of partially PCR-amplified DNA, 4.41 µL of nuclease-free H_2O, 0.25 µL of 25 µM Ad1_noMX primer, 0.25 µL of 25 µM Ad2.* indexing primer, 0.09 µL of 100× SYBR Green I (Cat. No. S-7563), 5 µL of NEBNext High-Fidelity 2× PCR Master Mix (Cat. No. M0541) with the following cycles: 1 cycle: 30 s at 98 °C and 20 cycles: 10 s at 98 °C, 30 s at 63 °C, 1 min at 72 °C. The additional number of PCR cycles (*N*) is the cycle that corresponds to one-third of the maximum fluorescent intensity. After determining the additional PCR cycles required, the remaining 45 µL of transposed DNA was further amplified with the following cycles: 1 cycle: 30 s at 98 °C and *N* cycles: 10 s at 98 °C, 30 s at 63 °C, 1 min at 72 °C. ATAC-seq libraries were two-stage purified using AMPure XP beads: 0.5X and 1.3X. Libraries are eluted in 20 µL nuclease-free water. The size and pattern of the ATAC-seq libraries were assessed by 6% TBE-PAGE. The concentration of each library sample was measured by KAPA Library Quantification kit (Cat. No.: kk4824). All libraries were pooled and a final quality check was performed using Bioanalyzer High-Sensitivity DNA Analysis kit. Sequencing was carried out on Illumina HiSeq 4000 system.

The followings were the primers used in this study:

Ad1_noMX (5'-AATGATACGGCGACCACCGAGATCTACACTCGTCGGCAGCGTCAGATGTG-3');
Ad2.1_TAAGGCGA(5'-
CAAGCAGAAGACGGCATACGAGATTCGCCTTAGTCTCGTGGGCTCGGAGATGT-3');
Ad2.2_CGTACTAG (5'-
CAAGCAGAAGACGGCATACGAGATCTAGTACGGTCTCGTGGGCTCGGAGATGT-3');
Ad2.3_AGGCAGAA (5'-
CAAGCAGAAGACGGCATACGAGATTTCTGCCTGTCTCGTGGGCTCGGAGATGT-3')
Ad2.4_TCCTGAGC (5'-
CAAGCAGAAGACGGCATACGAGATGCTCAGGAGTCTCGTGGGCTCGGAGATGT-3')
Ad2.5_GGACTCCT (5'-
CAAGCAGAAGACGGCATACGAGATAGGAGTCCGTCTCGTGGGCTCGGAGATGT-3')
Ad2.6_TAGGCATG (5'-
CAAGCAGAAGACGGCATACGAGATCATGCCTAGTCTCGTGGGCTCGGAGATGT-3');
Ad2.7_CTCTCTAC (5'-
CAAGCAGAAGACGGCATACGAGATGTAGAGAGGTCTCGTGGGCTCGGAGATGT-3');
Ad2.8_CAGAGAGG (5'-

CAAGCAGAAGACGGCATACGAGATCCTCTCTGGTCTCGTGGGCTCGGAGATGT-3');
Ad2.9_GCTACGCT (5'-
CAAGCAGAAGACGGCATACGAGATAGCGTAGCGTCTCGTGGGCTCGGAGATGT-3')
Ad2.10_CGAGGCTG (5'-
CAAGCAGAAGACGGCATACGAGATCAGCCTCGGTCTCGTGGGCTCGGAGATGT-3').

SHAPE-MaP

SHAPE-MaP was performed as described elsewhere (7). Briefly, ES cells were washed once with phosphate buffered saline, followed by adding 900 μl fresh medium and 100 μl of neat DMSO or 100 mM 1M7 in DMSO. After immediate mixing, cells were incubated at 37 °C for 5 minutes. Then cells were harvested, and RNA was purified using RNeasy Mini Kit (Qiagen). The mutational profiling (MaP) reverse transcription was carried out with SuperScript II reverse transcriptase (Life Technologies) in 1× MaP buffer (50 mM Tris (pH 8.0), 75 mM KCl, 6 mM $MnCl_2$, 10 mM DTT and 0.5 mM dNTPs), using random primers. The cDNAs were amplified by PCR using *Xist*-specific primers and Q5 high-fidelity DNA polymerase (NEB). The amplified DNA fragments were gel purified and pooled together. Construction of high-throughput sequencing libraries and sequencing were carried out by Novogene. Information of primers used for reverse transcription and PCR amplification of Xist cDNA are available in supplementary materials (Supplementary Table S2).

RNA FISH, immunostaining and immuno-RNA FISH

RNA FISH, immunostaining and immuno-RNA FISH were carried out as previously described (8). Immunostaining for H3K27me3 was performed using a mouse monoclonal antibody (Abcam; ab6002; 1:500) with a secondary antibody conjugated with Alexa-647 (ThermoFisher; A-21236; 1:1000). Immunostaining for H2AK119ub was performed using a rabbit monoclonal antibody (Cell Signaling Technology; D27C4; 1:2000) with a secondary antibody conjugated with Alexa-647 (Abcam; ab150075; 1:1000). Immunostaining was followed by RNA FISH. The *Xist* RNA was detected with Sx9 probe, a P1 DNA construct containing a 40 kb genomic fragment covering the *Xist* gene. Nucleotide analogs used in probe labeling were Cy3-dUTP (Amersham, Cat# PA53022).

Plasmid constructs

A mouse *Ssb* cDNA clone was purchased from OriGene (MG206549) and the sequence of the cDNA was confirmed by Sanger sequencing (data not shown). A series of in-frame deletions of various functional domains of *Ssb* were generated by PCR amplification using Herculase II Fusion Enzyme (Agilent Technologies) followed by Gibson Assembly (NEB). The sequences of the cloned cDNA fragments were confirmed by sequencing (data not shown).

For rescue experiments, the plasmid constructs were transfected into a female 3F1 ES cells with *Ssb* stably knockdown. G418 (ThermoFisher) was used at 250 μg/ml to select for stably transfected cells. Single surviving colonies were picked and examined using RT-qPCR. The shRNA construct, which worked efficiently against *Ssb*, was not designed against the 3' UTR of the RNA. Therefore, the shRNA is against some of the rescue plasmid constructs. Nonetheless, transfecting the *Ssb* knockdown cells with the rescue plasmids should compensate the effect of *Ssb* knockdown and serve as a rescue assay to study the functional domains of La.

Microscopy and live-cell imaging

Wide-field fluorescent microscopy work was carried out on an Eclipse Ti microscope (Nikon) with a digital camera (Clara Series model C01, Andor).

Live-cell imaging was performed on a CorrSight spinning disk confocal system (FEI Company) equipped with an Orca R2 CCD camera (Hamamatsu). 1 day before imaging, 800K feeder-free ES cells were seeded on fibronectin-coated glass-bottom dishes (MatTec Corp). Prior to live-cell imaging, cells were washed with 1x PBS and replaced with imaging medium composing complete medium for differentiating ES cells with DMEM substituted with FluoroBrite DMEM (ThermoFisher). 1 μg/ml of doxycycline was supplemented to the imaging medium to induce *Xist* expression. For live-cell time-lapse video recording, cells were placed into the microscope cell culture chamber heated to 37 °C at least 1 hr before imaging. Imaging was carried out in a closed chamber maintained at 37 °C with 5% CO2 and 90% humidity. A 488-nm laser line (iChrome MLE-LFA) was set at 100% laser power. Images were acquired using a PlanApo 63x/ 1.4 N.A. oil-immersion objective (Zeiss) (heated to 37 °C) with standard filter sets. The exposure time was set at 200 ms. All live-cell time-lapse video recording, unless explicitly stated otherwise, was carried out in a 2-hr time span with a 2-min time interval. For each time point, a 10-μm thick Z-stack with a 1-μm interval was collected. Autofocus system (Focus Clamp) was used to minimize out-of-focus throughout the recordings. Time-lapse

imaging was started 1 hr after the addition of doxycycline for differentiating cells. All acquired images were processed and analyzed using ImageJ (4). Drift correction was applied to all time-lapse recordings.

In the “sunset” experiments, the snap-shot images of *Xist* signals in live cells were captured with an 800-ms exposure time at 100% laser power in 10-μm Z-stacks at 1-μm intervals.

Data analysis

For padlock SNP capture, we only selected the SNPs which were allelotyped in all 6 samples. A nucleotide position with a read count less than 10 was considered as undetected and its read count was set to 0. Read counts of all the SNPs from one gene were combined to calculate the allelotype of the gene. Genes known to escape XCI were removed. The allelotype of each gene is calculated as Log ((129 count +10) / (Cast count +10)). To avoid division by 0, we added a pseudocount of 10 to each read count. The sequencing data is available in sequence read archive (SRA, accession number PRJNA545157).

For ATAC-seq, we mapped 10 million reads from each sample onto the mouse genome (mm9) using bowtie2 (9). The sequencing depth of each sample was normalized to the total number of reads with a single best alignment position along the mouse genome outside of chromosome X. The alignment position of each read indicates the site of a transposon insertion event. The number of insertion sites along a given 1 mb region was counted and named as the “Cut Count” of the region. The sequencing data is available in SRA (accession number PRJNA545157).

For SHAPE-MaP, the data analysis software “ShapeMapper_v1.2” was downloaded from Dr. Kevin Weeks lab website (https://weeks.chem.unc.edu/software.html) (10). The recommended sample data set “shapemapper_example_data” (https://weeks.chem.unc.edu/software.html) was also downloaded for software test runs. The source code written in Python 2 was revised for Python 3 updates. The source code was also modified to calculate SHAPE reactivity using one control ($MutationRate^{1M7}$ - $MutationRate^{DMSO}$) instead of two controls (($MutationRate^{1M7}$ - $MutationRate^{DMSO}$) / $MutationRate^{Denatured}$). The following parameters were customly adjusted for the data analysis of this study: primerLength = 30; minDepth = 5,000; trimBothEnds = on. The rest parameters were kept the same as the default setting of the software. The software was used for counting mutation and generating the parameters used for RNA structure analysis. Other data analysis, such as profiled nucleotides, mutation rate profiles and principle component analysis, was performed using Perl and Python scripts built in-house. The in-cell SHAPE sequencing data is available in SRA (accession number PRJNA589511).

Supplemental Figures

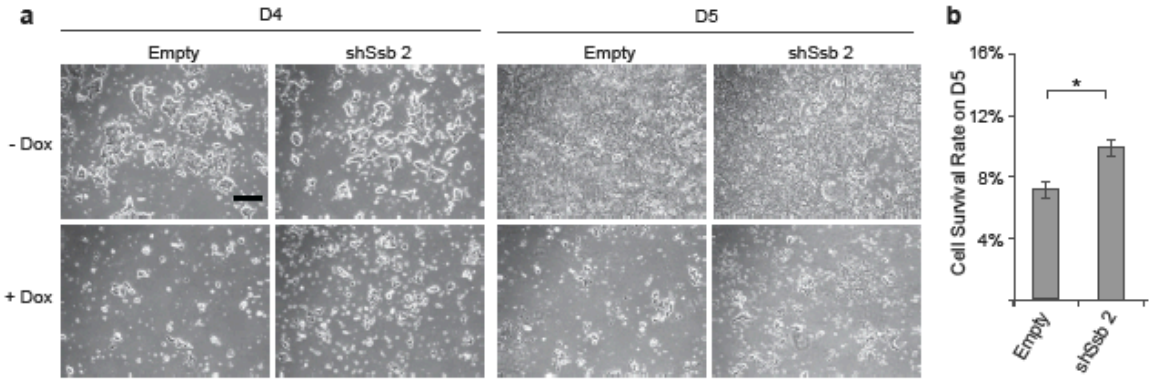

Figure S1: The effects of *Ssb* knockdown on the induced XCI in differentiating male ES cells. **(a)** Representative bright field microscope images of differentiating ES cell treated with Doxycycline for 4 and 5 days (D4 & D5). Clonal ES cell lines stably transfected with the shRNA constructs against *Ssb* and the empty shRNA vector are shown. Doxcycycline treatment was started upon *in vitro* differentiation. Scale bars, 300μm. **(b)** Cell survival rate was calculated by cell counting on day 5. Data are shown as mean ± SEM. The statistical analysis used is the Student's *t*-test. *p < 0.006; n = 3.

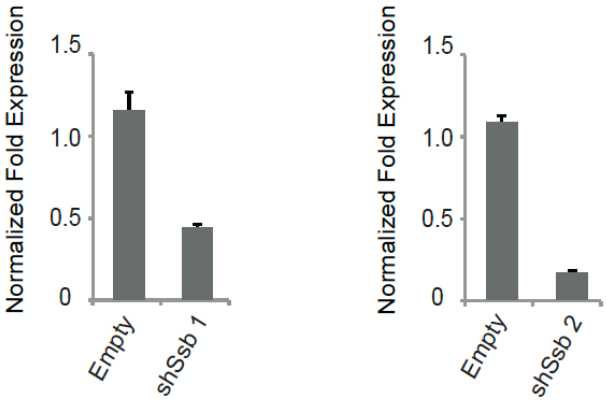

Figure S2: Quantitative RT-PCR to assess the effect of shRNA knockdown of *Ssb* in the female 3F1 cell lines. Data are shown in relative fold expression. Normalization was performed using Actb and Gapdh. Error bars indicate SEM (n = 3).

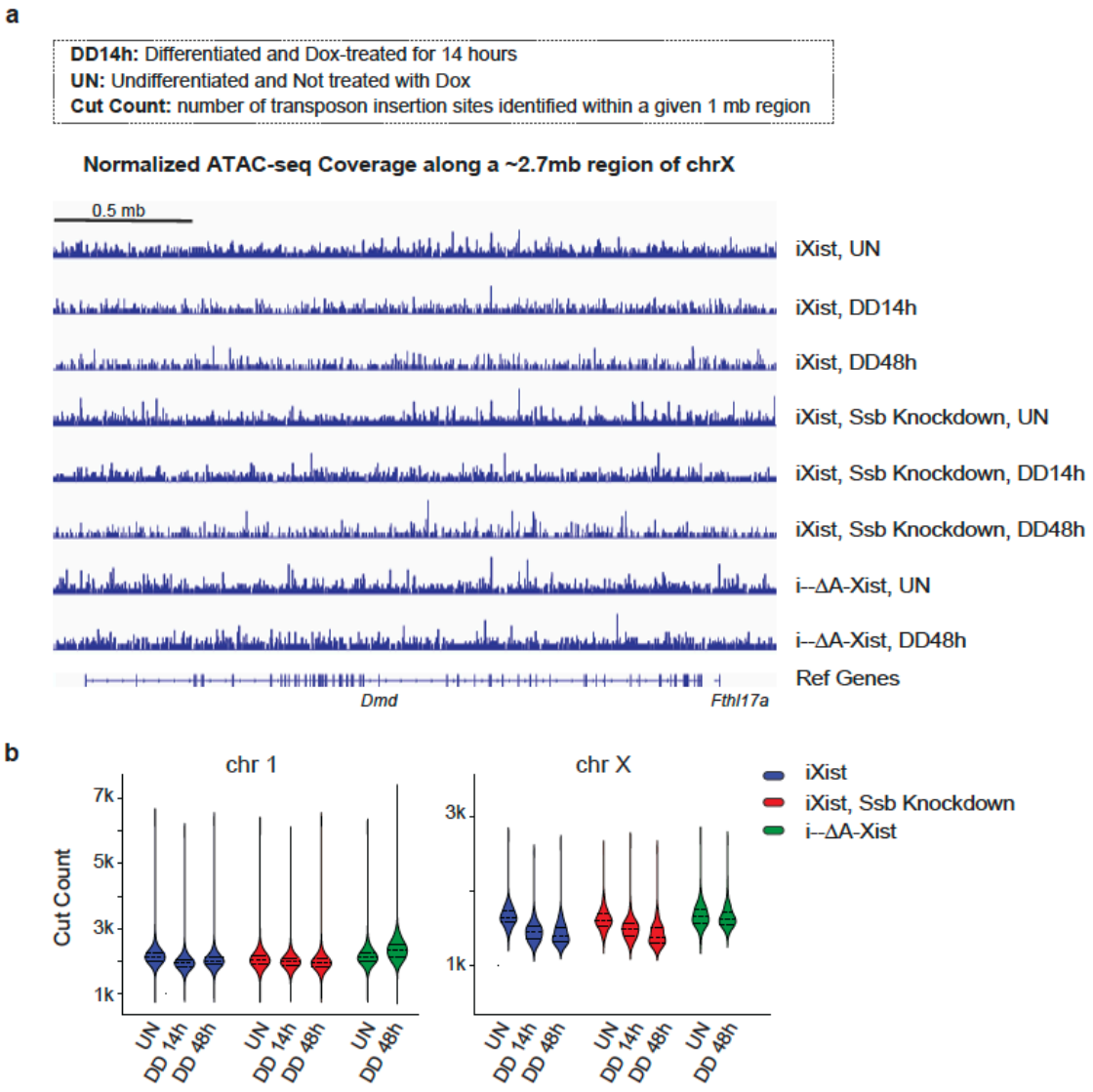

Figure S3: ATAC-seq results. (a) Normalized sequencing coverage along a ~2.7mb X-linked region. **(b)** The chromosomes are divided into 1-mb regions and the Cut Counts of each 1-mb region are shown in violin plots.

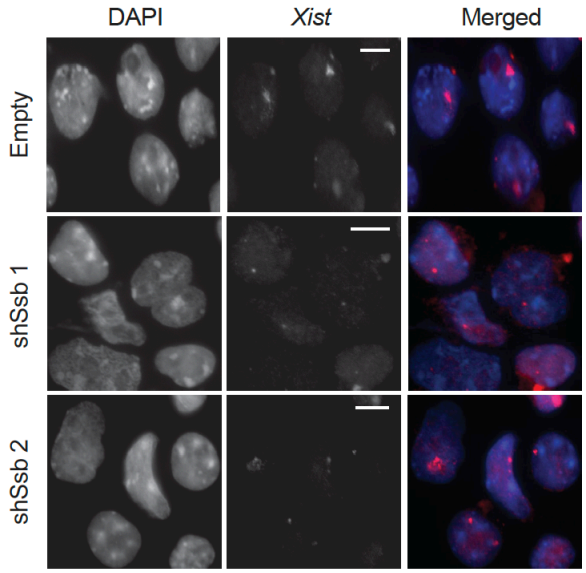

Figure S4: *Xist* RNA FISH results. The experiment was performed using day 6 *in vitro* differentiating female ES cells. DNA was counter stained with DAPI (blue). Scale bars, 8 μm.

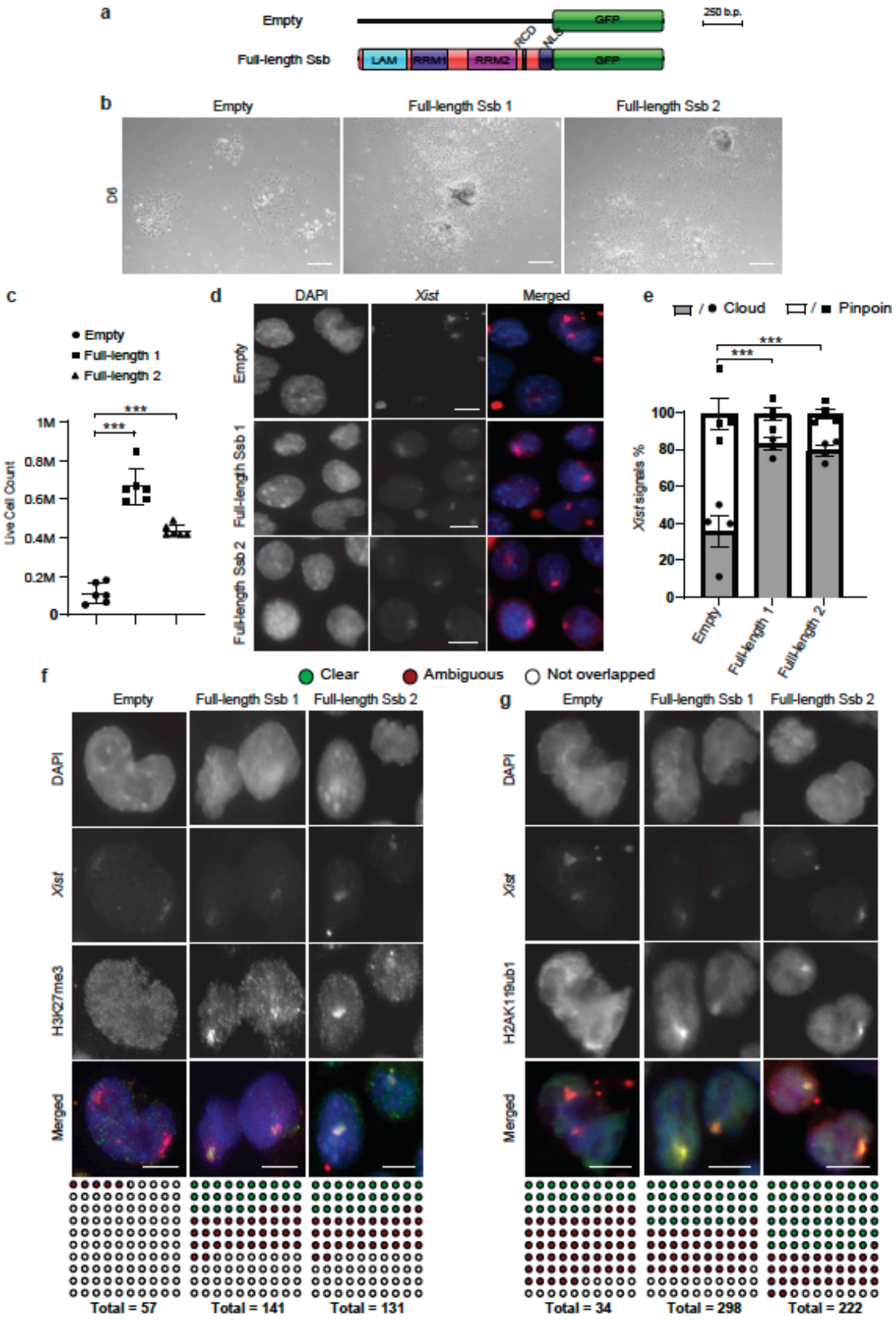

Figure S5: The rescue effects of full-length *Ssb* constructs on *Ssb* knockdown female cells during *in vitro* differentiation. (a) Diagram of the functional domains of La and the plasmid constructs. **(b)** Representative microscope images of day 6 differentiating ES cells. Scale bars, 300μm. Cells are clonal ES cell lines stably transfected with the corresponding plasmid constructs. **(c)** The rescue effects of full-length *Ssb* constructs on cell survival of *Ssb* knockdown cells during *in vitro*

differentiation. Cell counts of day 6 *in vitro* differentiation are shown. Data are shown as mean ± SEM (n = 6). The statistical analysis used is the Student's *t*-test. The data pairs with $p > 0.05$ (n.s.) are labeled. ***$p < 0.0001$. **(d)** *Xist* RNA FISH. DNA was counterstained with DAPI. Scale bars, 8μm. **(e)** Quantification of *Xist* RNA FISH signals. Data are shown as mean ± SEM (n = 243 for Empty; n = 545 for Full-length 1; n = 839 for Full-length 2). ***$p < 0.0001$ by X^2 test. **(f, g)** Immuno-RNA FISH detecting H2AK119ub, H3K27me3 and *Xist.* Cells were *in vitro* differentiated for 6 days. Immunostains were performed before the RNA FISH. DNA was counter stained with DAPI (blue). Scale bars, 8 μm. The total number of *Xist* clouds with clear, ambiguous or undetectable overlapping with the histone mark enrichment were tallied and tabulated below.

Table S1 *Xist*-binding proteins identified by “FLAG-out”

Nuclear Actin and Related Proteins		
ID	**Name**	**Also Identified in**
Q8VDD5	Myosin-9	
Q8BFZ3	Beta-actin-like protein 2	
Q9QXZ0	Microtubule-actin cross-linking factor 1	
Q80X90	Filamin-B	
Q9JI91	Alpha-actinin-2	
Q6URW6	Myosin-14	
Q9JMH9	Unconventional myosin-XVIIIa	
Q9JKF1	Ras GTPase-activating-like protein IQGAP1	
Q91Z67	SLIT-ROBO Rho GTPase-activating protein 2	
Q5NBX1	Protein cordon-bleu	
E9Q634	Unconventional myosin-Ie	
P59242	Cingulin	
P46735	Unconventional myosin-Ib	
Q8BQ30	Phostensin	
Q6R891	Neurabin-2	
Q8CI43	Myosin light chain 6B	
Q9Z2N8	Actin-like protein 6A	
Q9QXS6	Drebrin	
Q9R0P5	Destrin	
Q6P9R2	Serine/threonine-protein kinase OSR1	
Q61553	Fascin	
Q9WTI7	Unconventional myosin-Ic	
Q61879	Myosin-10	
Q8BTM8	Filamin-A	
Q64331	Unconventional myosin-VI	
Q9DBR7	Protein phosphatase 1 regulatory subunit 12A	
Q9ERG0	LIM domain and actin-binding protein 1	
Q9QYC0	Alpha-adducin	
Q9CVB6	Actin-related protein 2/3 complex subunit 2	
Q99JY9	Actin-related protein 3	
P14602	Heat shock protein beta-1	
Q2KN98	Cytospin-A	
P58774	Tropomyosin beta chain	
Q9QYB5	Gamma-adducin	
Q3THE2	Myosin regulatory light chain 12B	
O88990	Alpha-actinin-3	
O70318	Band 4.1-like protein 2	
Q9JJ28	Protein flightless-1 homolog	

Chromatin and Related Proteins		
ID	**Name**	**Also Identified in**
P62141	Serine/threonine-protein phosphatase PP1-beta catalytic subunit	
Q7TPV4	Myb-binding protein 1A	C, S
Q78ZA7	Nucleosome assembly protein 1-like 4	
O35129	Prohibitin-2	
O09106	Histone deacetylase 1	

Q99LL5	Periodic tryptophan protein 1 homolog	
P10853	Histone H2B type 1-F/J/L	
Q99J09	Methylosome protein 50	
Q60972	Histone-binding protein RBBP4	
Q62318	Transcription intermediary factor 1-beta	
P02301	Histone H3.3C	
Q9WTM5	RuvB-like 2	
P70168	Importin subunit beta-1	

DNA and RNA Binding Proteins		
ID	**Name**	**Also Identified in**
P17225	Polypyrimidine tract-binding protein 1	C, N
Q60817	Nascent polypeptide-associated complex subunit alpha	
Q8R4U7	Leucine zipper protein 1	
Q80U78	Pumilio homolog 1	
P11031	Activated RNA polymerase II transcriptional coactivator p15	
Q9CY58	Plasminogen activator inhibitor 1 RNA-binding protein	
Q921F2	TAR DNA-binding protein 43	C, S
P53996	Cellular nucleic acid-binding protein	
Q921M3	Splicing factor 3B subunit 3	
Q9DBD5	Proline-, glutamic acid- and leucine-rich protein 1	
P26369	Splicing factor U2AF 65 kDa subunit	
Q8K3Y3	Protein lin-28 homolog A	C
Q9CQF3	Cleavage and polyadenylation specificity factor subunit 5	
Q3U1J4	DNA damage-binding protein 1	
Q99KP6	Pre-mRNA-processing factor 19	
Q60865	Caprin-1	
Q02248	Catenin beta-1	
Q8BG81	Polymerase delta-interacting protein 3	C
P97855	Ras GTPase-activating protein-binding protein 1	
P32067	Lupus La protein homolog	C

Membrane Proteins		
ID	**Name**	**Also Identified in**
P39447	Tight junction protein ZO-1	
Q9Z0U1	Tight junction protein ZO-2	
P48962	ADP/ATP translocase 1	
Q68FD5	Clathrin heavy chain 1	
P23242	Gap junction alpha-1 protein	
Q9WVE8	Protein kinase C and casein kinase substrate in neurons protein 2	
P17809	Solute carrier family 2, facilitated glucose transporter member 1	
Q7TMK6	Protein Hook homolog 2	

Nuclear RNP; Ribosomal or Nucleolar Proteins		
ID	**Name**	**Also Identified in**
P47962	60S ribosomal protein L5	
P35980	60S ribosomal protein L18	

P62911	60S ribosomal protein L32	
P62267	40S ribosomal protein S23	
O09167	60S ribosomal protein L21	
P62862	40S ribosomal protein S30	
P62717	60S ribosomal protein L18a	
P12970	60S ribosomal protein L7a	
P41105	60S ribosomal protein L28	
P47911	60S ribosomal protein L6	
P62855	40S ribosomal protein S26	
P61514	60S ribosomal protein L37a	
P47915	60S ribosomal protein L29	
P14148	60S ribosomal protein L7	
P53026	60S ribosomal protein L10a	
Q9D8E6	60S ribosomal protein L4	
P62242	40S ribosomal protein S8	
P14206	40S ribosomal protein SA	
P47963	60S ribosomal protein L13	
P63276	40S ribosomal protein S17	
P47964	60S ribosomal protein L36	
P62892	60S ribosomal protein L39	
Q9D0E1	Heterogeneous nuclear ribonucleoprotein M	C, N, S
Q9Z2X1	Heterogeneous nuclear ribonucleoprotein F	
Q60668	Heterogeneous nuclear ribonucleoprotein D0	C
Q8VEK3	Heterogeneous nuclear ribonucleoprotein U	C, N, S
Q61937	Nucleophosmin	
Q9CPP0	Nucleoplasmin-3	
O54825	Bystin	
Q62189	U1 small nuclear ribonucleoprotein A	

Other Proteins		
ID	**Name**	**Also Identified in**
O70251	Elongation factor 1-beta	
O54931	A-kinase anchor protein 2	
Q9D8W5	26S proteasome non-ATPase regulatory subunit 12	
O88844	Isocitrate dehydrogenase [NADP] cytoplasmic	
O88735	Ensconsin	
Q9R0Q9	Mannose-P-dolichol utilization defect 1 protein	
Q61316	Heat shock 70 kDa protein 4	
Q9JKV1	Proteasomal ubiquitin receptor ADRM1	
Q8BFR5	Elongation factor Tu, mitochondrial	
Q9CZS1	Aldehyde dehydrogenase X, mitochondrial	
Q8BJM7	S-adenosyl-L-methionine-dependent tRNA 4-demethylwyosine synthase	
P45376	Aldose reductase	
P23116	Eukaryotic translation initiation factor 3 subunit A	
P26516	26S proteasome non-ATPase regulatory subunit 7	
P17751	Triosephosphate isomerase	
O88685	26S protease regulatory subunit 6A	
P05064	Fructose-bisphosphate aldolase A	
P68040	Guanine nucleotide-binding protein subunit beta-2-like 1	

Q9D4J1	EF-hand domain-containing protein D1	
Q8QZY1	Eukaryotic translation initiation factor 3 subunit L	
Q8JZQ9	Eukaryotic translation initiation factor 3 subunit B	
P60229	Eukaryotic translation initiation factor 3 subunit E	
P35700	Peroxiredoxin-1	
P17182	Alpha-enolase	
Q91VJ4	Serine/threonine-protein kinase 38	
P24369	Peptidyl-prolyl cis-trans isomerase B	
Q3TXS7	26S proteasome non-ATPase regulatory subunit 1	
P99024	Tubulin beta-5 chain	
P01868	Ig gamma-1 chain C region secreted form	

Table S2. Primers for PCR amplification of Xist cDNAs in SHAPE-MaP.

Amplicon name	**Forward primer**	**Reverse primer**
*Xist*_21	GCTTGGTGGATGGAAATATGG	CGTTATACCGCACCAAGAAC
*Xist*_20	AGCGGACTGGATAAAAGCAAC	CATCACAGTCTAATTCCATCCTG
*Xist*_19	TGTTGGTGTTTGCTTGACTTCC	AAACTTTAAGGACTCCAAAGTAAC
*Xist*_18	CGTCTGATAGTGTGCTTTGC	GGCTTGGGATAGGTCTGAAA
*Xist*_16	CCCATCTATACCCCCTCCAT	GCAAGGGTAGTATTAGGACCTTGAG
*Xist*_15	TCACATGCTTTCTTATTTCAGCC	AGTTAACACTGTGCACATTTAC
*Xist*_14	GGTTCCTACCACTATGCCCTG	AAAACCCCATCCTTTATGCAA
*Xist*_12	AGCAGAAAGAGGGTTGTACG	TGATGGAATTGAGAAAGGGCAC
*Xist*_11	TCCATTGACCACTTTTCTGAATCAC	AAGATACTTGTCTTAAACATTCTGC
*Xist*_10	TACTGAGGGTGATGAGTCTGT	TCAGCAATGTCATATCAAACAC
*Xist*_8	ACAAAAAGCTTACAGGCCACA	AATAGACACAAAGCAAGGAAG
*Xist*_6	GTCTCCTTGTGTTGTCTAATTCG	TTCTGGACCTATTGGGAAGGG
*Xist*_4	CCCAGCATCCCTTTCCATTTC	AATTGCCAATGTGCTATGAG
*Xist*_3	AGGACTACTTAACGGGCTTA	AGGGTAATCAATCACCTGCA
*Xist*_-1	GAGACATGGTCTCATAAAGCC	TGTGTGGAACCGAGGAAATA
*Xist*_-3	TAGGCCATTTTAGCTATGACTGT	TTTGAACTCCCAGACCTCTTC

Movies S1-3: The emergence of induced *Xist* RNA signals in wild type differentiating ES cells.
Movies S4-7: The emergence of induced *Xist* RNA signals in *Ssb* mutant differentiating ES cells.

Supplementary References

1. C. Chu*, et al.* Systematic discovery of Xist RNA binding proteins. *Cell.* 161, 404-416 (2015).
2. C.A. McHugh*, et al.* The Xist lncRNA interacts directly with SHARP to silence transcription through HDAC3. *Nature.* 521, 232-236 (2015).
3. A. Minajigi*, et al.* Chromosomes. A comprehensive Xist interactome reveals cohesin repulsion and an RNA-directed chromosome conformation. *Science.* 349, 2015).
4. C.A. Schneider, W.S. Rasband, & K.W. Eliceiri. NIH Image to ImageJ: 25 years of image analysis. *Nat Methods.* 9, 671-675 (2012).
5. R. Hong*, et al.* High-resolution RNA allelotyping along the inactive X chromosome: evidence of RNA polymerase III in regulating chromatin configuration. *Sci Rep.* 7, 45460 (2017).
6. J.D. Buenrostro, B. Wu, H.Y. Chang, & W.J. Greenleaf. ATAC-seq: A Method for Assaying Chromatin Accessibility Genome-Wide. *Curr Protoc Mol Biol.* 109, 21 29 21-29 (2015).
7. M.J. Smola*, et al.* SHAPE reveals transcript-wide interactions, complex structural domains, and protein interactions across the Xist lncRNA in living cells. *Proc Natl Acad Sci U S A.* 113, 10322-10327 (2016).
8. L.F. Zhang, K.D. Huynh, & J.T. Lee. Perinucleolar targeting of the inactive X during S phase: evidence for a role in the maintenance of silencing. *Cell.* 129, 693-706 (2007).
9. B. Langmead & S.L. Salzberg. Fast gapped-read alignment with Bowtie 2. *Nat Methods.* 9, 357-359 (2012).
10. M.J. Smola, G.M. Rice, S. Busan, N.A. Siegfried, & K.M. Weeks. Selective 2'-hydroxyl acylation analyzed by primer extension and mutational profiling (SHAPE-MaP) for direct, versatile and accurate RNA structure analysis. *Nat Protoc.* 10, 1643-1669 (2015).